Thermal and Structural Properties of Poly(Vinyl Alcohol) Doped with Hydroxypropyl Cellulose

N. A. El-Zaher,[1] W. G. Osiris[2]

[1]*National Institute for Standards, Giza, Egypt*
[2]*Biophysics Department, Faculty of Science, Cairo University, Giza, Egypt*

Received 24 February 2004; accepted 27 August 2004
DOI 10.1002/app.21628
Published online in Wiley InterScience (www.interscience.wiley.com).

ABSTRACT: The growth and importance of medical and related health care and hygiene textile sectors are attributed to the improvement and innovations in both textile technology and medical procedures. The aim of this study was to examine some of the structural properties of pure poly(vinyl alcohol) (PVA) and hydroxypropyl cellulose (HPC) doped PVA of different weight percentages. This will lead to the choice of the optimum conditions suited for specific medical and surgical applications for which textile materials are currently used. Thermogravimetry was used to develop an instrumental system for the study of thermal stability and for identification of the individual components of several polymer blends. Derivative thermogravimetry provided clear information and distinguished between different generic types. Also, differential scanning calorimetry and its derivatives gave accurate values of glass-transition temperature and melting temperature and gave detailed features of the steps of weight loss and changes in the heat of fusion. The X-ray diffraction technique was used to determine the crystallinity/amorphosity ratio and the change in crystallite size at different dopant concentrations. The effect of doping with HPC on PVA structure was studied with spectrophotometric analyses. Variations in the group coordination in the IR region were followed. The data obtained indicated that measurable and remarkable changes in the thermal stability of PVA occurred at different doping concentrations. This may have been because the diffusion of dopant caused structural changes in the polymer matrix. © 2005 Wiley Periodicals, Inc. J Appl Polym Sci 96: 1914–1923, 2005

Key words: poly(vinyl alcohol); hydroxypropylcellulose; thermogravimetry; differential scanning; calorimetry; X-ray diffraction; spectrophotometric analyses

INTRODUCTION

Textile materials and products that have been engineered to meet particular needs are suitable for many medical and surgical applications in which a combination of strength, flexibility, and sometimes moisture and air permeability is required. Materials used include monofilament and multifilament yarns; woven, knitted and nonwoven fabrics; and composite structures. The applications are many and diverse, ranging from a single-thread suture to composite structures used for bone replacement and from a simple cleaning wipe to the advanced barrier fabrics used in operating rooms.[1,2]

Poly(vinyl alcohol) (PVA; —[—CH_2—CHOH—]$_n$—) is the world's largest volume synthetic polymer produced for its excellent chemical resistance and physical properties and complete biodegradability, which has led to broad practical application. PVA is a water-soluble polyhydroxy polymer, one of the few linear, nonhalogenated aliphatic polymers. PVA has a two-dimensional hydrogen-bonded network sheet structure. The sheets are stacked and bonded together by weak Van der Waal's forces.[3–5] The physical and chemical properties of PVA depend to a greater extent on the method of preparation than is ordinarily the case with other polymers. PVA has good mechanical properties when it is in a dry state, but its application is limited by its high hydrophilicity.[6,7] Chemical crosslinking may improve its mechanical properties and antiwater solubility.[8] PVA is largely applied in surgical devices, hybrid islet transplantation, implantation,[9,10] and a synthetic articular cartilage in reconstruction joint surgery.[11]

Nanoscale diameter PVA, produced by an electrospinning process through the action of an external electric field imposed on a polymer solution or melt,[12] has a large specific surface area and a small pore size, making it excellent for use in filtration, biomedical materials,[13] and membrane applications. PVA gels are used as tissue phantoms in photoacoustic applications, so it must possess both optical and acoustic properties of human tissue. PVA properties have been measured to be close to the average properties of human breast tissue. Moreover, PVA may be used in sheets to make bags for premeasured soap for washing machines or the larger bags used in hospitals as

Correspondence to: W. G. Osiris (osiris_wgr@yahoo.com).

containers for cotton cloth used in operating rooms or for the clothing of infected patients.

The modification of PVA with aldehydes, carboxylic acid, and anhydrides increases membrane selectivity and fiber manufacture among other things.[14,15] The esterification of PVA leads to water-insoluble hydrophilic vinyl alcohol/vinyl ester copolymers with a structure that can be used, for example, as a support for sustained delivery of water-soluble bioactive compounds.[16]

In recent years, copolymers and blends have attracted the attention of material researchers to obtain intermediate properties with respect to homopolymers for some specific functions. These interesting properties are attributable to the molecular motions allowed in their amorphous phases. The interphase regions in blends and copolymers are very important. Depending on the chemical nature of the doping substances and the type and extent in which they interact with host matrix, the dopant alters the physical properties to different degrees.[17–19] Considerable interest has been shown in the effect of doping on the transport properties of polymers.

In this investigation, an aqueous blend of two polar and hydrogen-bonding-group-containing polymers, PVA and hydroxypropyl cellulose (HPC), was studied. The compatibility of the two polymers in the solid state was followed by means of thermal properties with thermal analysis techniques: ratio crystallinity/amorphosity, crystallite size change as studied with X-ray diffraction (XRD), transmission properties in the IR region as studied with Fourier transform infrared (FTIR) analysis, and properties as studied by visual inspection for pure PVA and HPC-doped PVA with different weight percentages (4–16 wt %).

EXPERIMENTAL

PVA (Poval 250) granules was supplied from El-Nasr Co. (Cairo, Egypt). HPC was supplied by Shin Etsu Chemical Co. (Tokyo, Japan).

The solution method[20] was used to obtain film samples. This method depended on the dissolution of weighed amounts of the PVA granules in double-distilled water. Complete dissolution was obtained with a magnetic stirrer in a 50°C water bath. Weighed amounts of HPC powder were dissolved in double-distilled water in a 50°C water bath. To prepare thin films of pure PVA and doped with HPC, we mixed the solutions together at 50°C with different weight percentages (4–16%) with a magnetic stirrer. Thin films of an appropriate thickness (0.01 cm) were cast onto stainless steel Petri dishes (10 cm in diameter) and were dried in air at room temperature (ca. 25°C) for 7 days until the solvent was completely evaporated. Films were cut into slabs of suitable dimensions for each measurement.

The thermal behaviors of pure PVA and the HPC-doped PVA samples were investigated with a Shimadzu TGA-50 (Kyoto, Japan) for thermogravimetric analysis (TGA). The thermogravimetric curves were differentiated with respect to time concurrently with an analogue-derivative unit. A Shimadzu DSC-50 analyzer (Kyoto, Japan) was used for differential scanning calorimetry (DSC). DSC experiments were carried out on all samples at a heating rate of 10°C/min, with dry nitrogen (N_2) as the carrier gas, and at a flow rate of 30 mL/min. Sample runs were repeated at least three times to ensure reproducibility. Scans were started at temperature of 30°C and run to a final temperature of 400°C.

A Scintag Irc X-ray diffractometer with Cu Kα radiation was used. It operated at 45 kV and 40 mA, with a wavelength (λ) of 1540.6 Å. The diffractograms were recorded continuously in the range $2\theta = 5–60°$ at a scanning rate of 2°/min. The relation of Segal et al.[21] was used to compute the crystallinity index (CrI) for pure PVA and the HPC-doped PVA samples as

$$\mathrm{CrI} = [I_t - I_s)/I_f] \times 100$$

where I_f is the peak intensity of the fundamental band at $2\theta = 17.0–18.5°$ and I_s the peak intensity of the secondary band at $2\theta = 6–8°$. The CrI is a time-save empirical measure of relative crystallinity.

The IR transmittance spectra were recorded with a PerkinElmer FTIR spectrophotometer (model 1650) (TX) in the wave number range 4000–500 cm^{-1}. The changes in some chemical groups' content were monitored with transmitted IR at selected bands.

RESULTS AND DISCUSSION

Thermal analyses

Thermogravimetry (TG) provided quantitative information on the weight change process. Figure 1 shows TGA curves for pure PVA, pure HPC, and the HPC-doped PVA samples at different concentrations. The recorded thermogravimetric plots for all samples showed two degradation steps, which suggested the coexistence of more than one degradation process. The lower temperature loss (i.e., the first step) may have corresponded to the breaking of ester linkages, and the second may have corresponded to the degradation of the whole polymer. The second loss was the most important, both in the rate of weight loss and in the total weight loss. If PVA was heated above 120°C, water was eliminated to give conjugated double bonds, and it could give a formation of ether crosslinks; that is, on heating PVA above the decomposition temperature, the polymer began a rapid chain-stripping elimination of H_2O.[22,23] In the case of pure polymeric fabrics, the first step can be assigned to

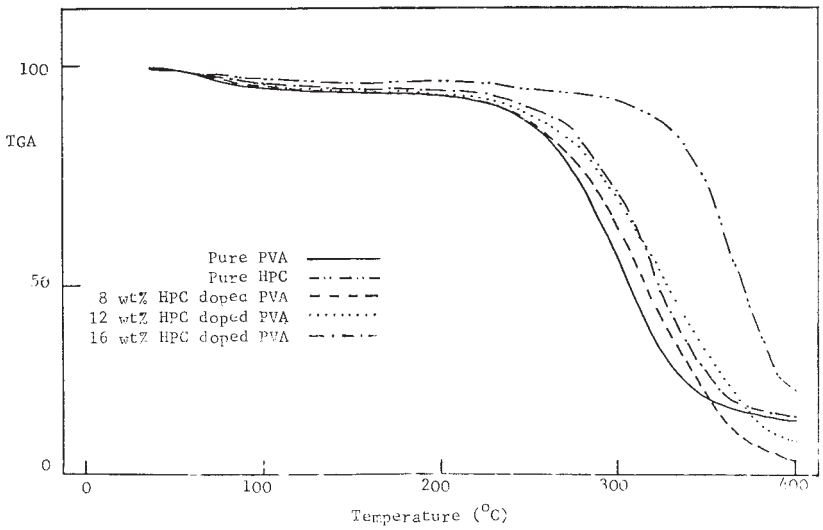

Figure 1 Typical TGA thermograms of pure PVA, pure HPC, and the HPC-doped PVA samples.

thermooxidative degradation, which is transformed to carbonaceous residues. These may decompose during the second step of the degradation process.

Cryghton and Holmes[24] expressed the opinion that TG has potential as a technique for polymer characterization (especially in the form of fibers). Chiu[25] found that the temperature at which mass loss starts and proceeds at its fastest rate is unique for any given polymer (the second step in our investigation), and the technique can be used for characterization purposes.

Figure 2 represents a relation between weight loss percentage for pure PVA, pure HPC, and the HPC-doped PVA samples for the first and second transition steps and the total weight loss as a function of dopant concentration. No remarkable change was seen in the first-step weight loss, whereas in the second step and also the total weight loss, there were small decreases up to concentrations of 8 wt % HPC followed by a rapid decrease at 12 wt % HPC and then an increase at 16 wt % HPC, where it reached the value of the pure PVA sample. This meant that PVA became more thermally stable when doped with 12 wt % HPC.

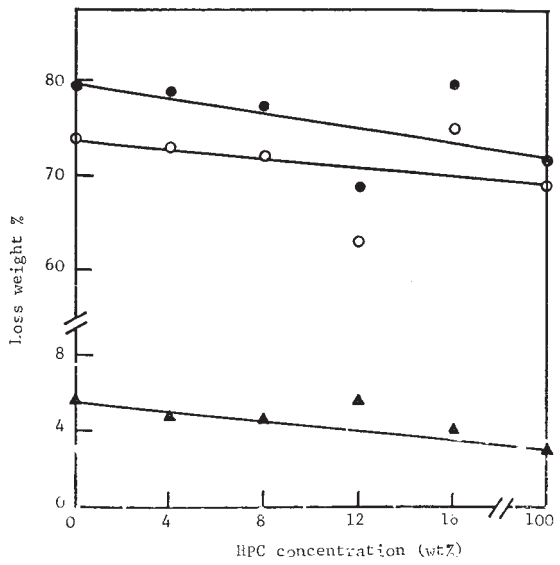

Figure 2 Relation between weight loss percentage and HPC dopant concentration: (▲) first, (○) second, and (●) total weight loss percentages.

It is difficult to identify very small or overlapping mass changes with blends. So, the determination of the first derivative of the mass loss curve (TGA) by the plotting of the rate of mass loss against time or temperature converts the loss steps to peaks, and subtle features of the original curve become clearer. Derivative thermogravimetric analysis (DTGA) traces for pure PVA, pure HPC, and the HPC-doped PVA samples of different concentrations are shown in Figure 3. Table I indicates the values of the glass-transition temperature (T_g) and the melting temperature (T_m) and their percentage changes for the samples detected from Figure 3. T_g values for the PVA ranges from 60 to 85°C depend on PVA's molecular weight and purity.[26,27] In addition, T_m is affected by polymer morphology, and a high crystallinity of a polymer means a high T_m. It is clear from Table I that a maximum increase in the T_m was obtained for 12 wt % HPC-doped PVA, which supported the thermal stability of PVA as previously mentioned.

On the other hand, it is also clear from Table I that T_g for pure PVA was 63.21°C and the T_g for pure HPC was 55.80°C, so it was difficult to analyze T_g for the HPC/PVA blends. Therefore, the difference in T_g between the two blend components was insufficient to support homogeneous blend morphology by that analysis, and to rule out transitional overlapping will not hamper the observation of separate T_g values.[28] The difference in the T_g values of the PVA and HPC

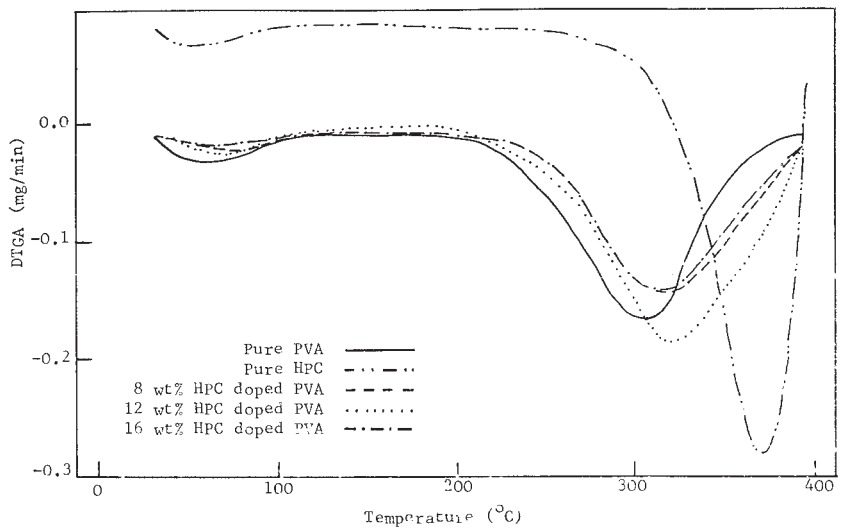

Figure 3 Recorded DTGA thermograms of pure PVA, pure HPC, and the HPC-doped PVA samples.

components was only about 8.6°C. We did not expect that two separate transition temperatures would be resolved. However, to obtain information concerning the state of the HPC/PVA blend, it is enough to analyze the actual transition temperature rather than the shape of the transition. If T_g values of the doped polymer is intermediate between those of the parent polymers, this means that it is a miscible polymer blend. They follow such models as the Gordon–Taylor or Fox relationships.[29,30] However, in the case of the HPC/PVA blends, the T_g data did not follow any of these well-known models. T_g of doped PVA was above those of the parent polymers (Table I).

Figure 4 shows the DSC curves for pure PVA, pure HPC, and the HPC-doped PVA samples in different concentrations. The difference in the shape and area of the melting endotherms were noticed. Pure PVA had a broader endotherm than that of 8 wt % HPC dopant PVA, which was sharp and had less area under the peak. The area became larger and broader at 12 wt % HPC, and again a decrease in the area and a little sharpness occurred in the 16 wt % HPC-doped sample. This variation in shape was attributed to the different degrees of crystallinity found in the samples with different dopant concentrations.[31] Peaks broadened as OH content declined. The PVA hydroxyl groups were highly interconnected by hydrogen bonding, leading to high T_g's. The introduction of other functional groups (e.g., HPC groups in our case) may have supported this bonding and enhanced the T_g value to a maximum in the 12 wt % HPC-doped sample. Also, a reduction in the peak area indicated a change in the extent of crystallinity or in the organization.[32] On other hand, a decrease in enthalpy of fusion and increase in T_m suggested that the crystallinity and perfection of the crystal structure were reduced with increasing degree of crosslinking. A change in the crystalline structure could have resulted from polymer–polymer (PVA and HPC) interactions in the amorphous phase. So, disorder in the crystals was created, reducing the enthalpy of the phase change.[33,34] The observed change in endotherm area may have indicated the existence of polymer–polymer interactions between HPC and PVA molecules. The area under the melt endotherm of the DSC thermograms [Fig. 4; i.e., heat of fusion (J/g)] of PVA, HPC, and HPC-doped PVA is given in Table II. It is clear that heat of fusion changed significantly as the HPC concentration increased. These changes were attributed to a variation in crystallization.

Typical derivative differential scanning calorimetry (DDSC) thermograms for pure PVA, pure HPC, and the HPC-doped PVA samples are shown in Figure 5. The DDSC results show that pure PVA and the HPC-doped PVA samples had six regions with different rates of mass

TABLE I
Values of T_g and T_m and Their Percentage Changes for the Pure PVA, Pure HPC, and HPC-Doped PVA Samples

Sample	T_g (°C)	ΔT_g[a] (%)	T_m[b] (°C)	ΔT_m (%)
Pure PVA	63.21	—	306.11	—
4 wt % HPC-doped PVA	79.01	25.0	312.12	2.0
8 wt % HPC-doped PVA	77.02	21.8	317.17	3.6
12 wt % HPC-doped PVA	74.20	17.4	323.69	5.7
16 wt % HPC-doped PVA	71.08	12.5	317.69	3.8
Pure HPC	55.80	—	371.06	—

$$^{a}\Delta T_g\ (\%) = \frac{(T_g)\ \text{doped PVA} - (T_g)\ \text{pure PVA}}{(T_g)\ \text{pure PVA}} \times 100$$

$$^{b}\Delta\ T_m\ (\%) = \frac{(T_m)\ \text{doped PVA} - (T_m)\ \text{pure PVA}}{(T_m)\ \text{pure PVA}} \times 100$$

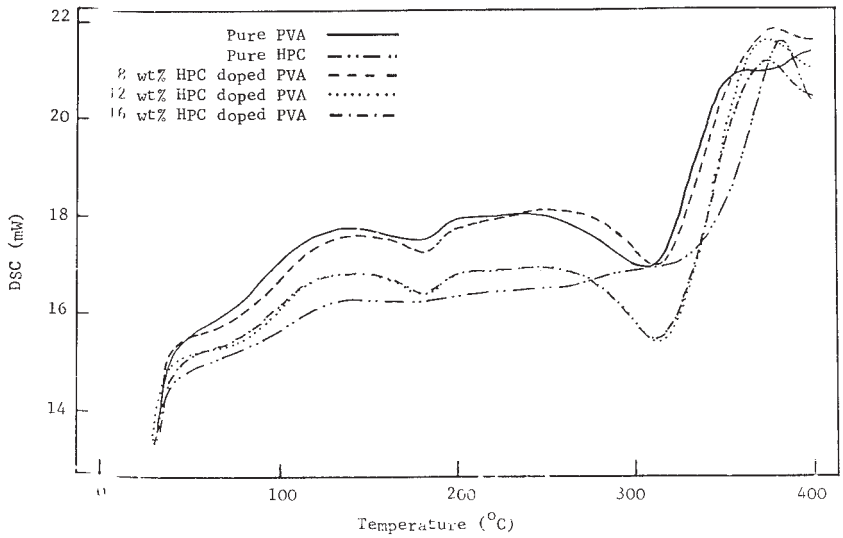

Figure 4 DSC curves for pure PVA, pure HPC, and the HPC-doped PVA samples.

loss, whereas DDSC for pure HPC indicated seven transition steps until complete decomposition was reached. The aforementioned steps did not show distinct peaks in the TGA curves. Mass loss started at 32–38°C, and there were clear single peaks at 171–173, 189–192, 296–300, and 338–343°C. Mass loss was completed at 384–392°C. For 8 wt % HPC, the appearance of a shoulder toward the left near the top of the peak at 340.5°C and another shoulder toward the light near the midheight of this peak were observed, which means that the average size of crystallites changed due to doping.

XRD analysis

The main physical properties of polymers (including their mechanical properties) are strongly dependent on the amount and nature of their crystalline and amorphous regions, that is, not only on the chemical structure but also on supermolecular organization. Also, this amount is responsible for chemical reactions, the absorbitivity of dyes and pigments, and humidity in the case of polymeric fabrics. The larger the amorphous part of the polymer is, the higher its reactivity will be.[35]

XRD has been used by many researchers to characterize changes in the crystal structure parameters, including the degree of crystal orientation, the apparent crystal size, and the lattice strain along the axis of the crystal unit cell.[36] Analysis of these diffractions yields a great deal of valuable information on the configuration of macromolecules and the size of the ordered regions of the material.

XRD was used to check the crystalline formation[37] of pure PVA and PVA samples doped with different weight percentages of HPC. Their typical XRD patterns are represented in Figure 6. There was a noticeable change in the intensity of the XRD peaks of the doped sample, and additional peaks appeared. Band intensities for the peaks are shown in Figure 7. Two distinguished bands were centered at 2θ = 6.88–7.68° and 2θ = 17.27–18.41°. From the patterns, we noted that new bands started to appear at 2θ = 11.34, 16.82, 25.83, 28.86, and 39.50° for the HPC-doped PVA samples at concentrations of 12 and 16 wt %. As doping increased, the extra peaks started growing and became major peaks in the largely doped samples. By following all of the bands intensities at different 2θ values, we noticed that band intensities increased con-

TABLE II
Values of Transition Temperature and Heat of Fusion for the Pure PVA, Pure HPC, and HPC-Doped PVA Samples

Sample	Transition temperature (°C)	Heat of fusion (J/g)	Transition temperature (°C)	Heat of fusion (J/g)	Transition temperature (°C)	Heat of fusion (J/g)
Pure PVA	77.66	−29.88	179.16	−42.10	305.81	−583.68
PVA + 8 wt % HPC	80.55	−69.60	180.65	−40.38	311.20	−484.00
PVA + 12 wt % HPC	83.86	−53.47	181.70	−33.44	312.78	−665.90
PVA + 16 wt % HPC	83.73	−42.42	180.12	−37.51	310.35	751.79
Pure HPC	41.68	78.75	134.90	57.00	383.01	143.36

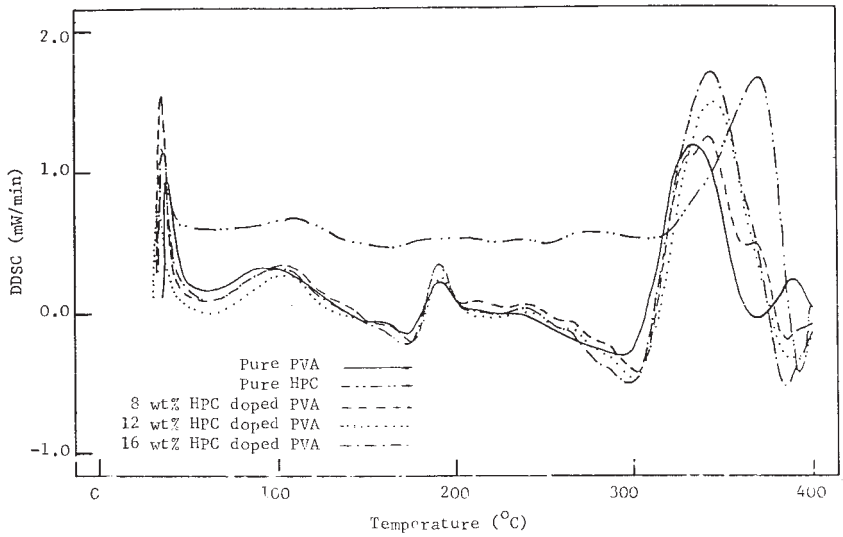

Figure 5 Recorded DDSC curves for pure PVA, pure HPC, and the HPC-doped PVA samples.

tinuously with increasing HPC dopant concentration up to 12 wt %; then, it drops drastically for PVA + 16 wt % HPC. The percentage increase and decrease with respect to the pure PVA band intensity values for the fundamental peak (2θ = 17.9–18.5°) are shown in Table III.

Figure 8 shows the relation between the half-bandwidth of the X-ray patterns versus the dopant concentration of HPC for the fundamental band at 2θ = 17.0–18.5°. It is clear from Figure 8 that there was a remarkable decrease in the half-bandwidth for the sample with 12 wt % HPC, which meant that crystallite size became larger (an inverse relation).[38] However, the broadening of the major peaks overlapped at 12 wt % HPC at 2θ = 17.00–18.41°. This band at 16 wt % HPC returned to be lower and sharper, although for the sample with 8 wt % HPC, this band split into two bands and had a shoulder at 2θ = 15.44°.

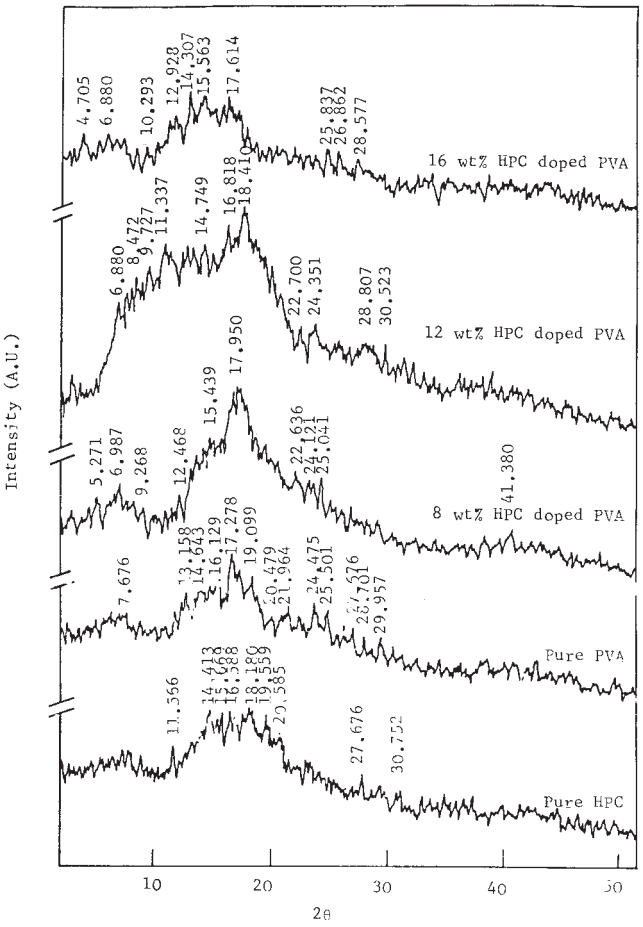

Figure 6 XRD patterns for pure PVA, pure HPC, and the HPC-doped PVA samples.

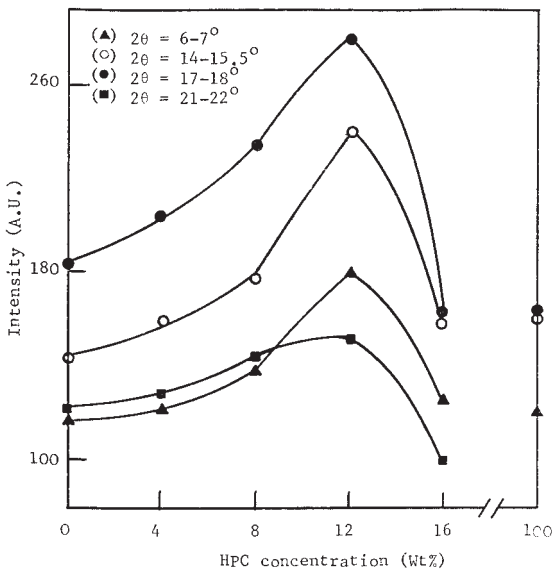

Figure 7 Band intensity of XRD patterns at different angles for pure PVA and the HPC-doped PVA samples.

TABLE III
Percentage Change in Intensity of the Fundamental Peak at $2\theta = 17.0–18.5°$

Sample	Percentage change in intensity
Pure PVA	—
4 wt % HPC-doped PVA	10.9
8 wt % HPC-doped PVA	26.6
12 wt % HPC-doped PVA	52.2
16 wt % HPC-doped PVA	−14.1

Crystallinity is defined as the weight fraction of the crystalline portion of a polymer. The physical and mechanical properties of polymers are considerably dependent on that parameter. XRD is most frequently used to measure crystallinity in polymers. The method is based on the assumption that it is possible to separate the intensity contributions arising from the crystalline and amorphous regions. The degree of crystallinity is the ratio of the integrated intensity under the crystalline peaks to the integrated intensity under the complete XRD trace. Other measures, such as peaks height, may be used. With proper attention to experimental detail, this method provides one of the fundamental measures of crystallinity in polymers.

Figure 9 shows the variation of CrI as a function of different concentrations of the dopant HPC on PVA, as calculated from the X-ray patterns (Fig. 6). CrI increased steeply, reaching a maximum value for the sample with 8 wt % HPC, and then dropped with increasing HPC concentration. The increase in CrI may indicate that there was an increase in crystalline regions, whereas its decrease meant that amorphosity dominated. This implies changes in the structural regularity of the main chains of the polymeric molecules on doping.

The results indicate that structural changes occurred in the polymer matrix as the dopant diffused. The hydroxyl ions of HPC were coordinated through hydrogen bonds, with the hydroxyl groups belonging to the different chains in PVA. A decrease in crystallinity has been proposed as one or another aspect of the

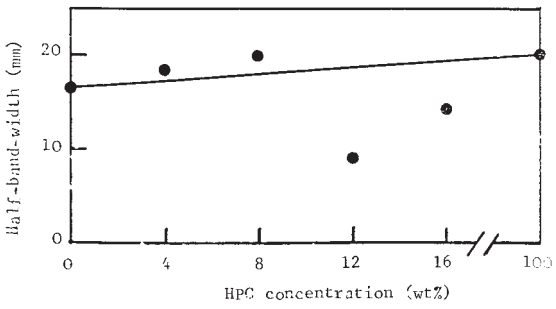

Figure 8 Relation between half-bandwidth of the X-ray bands versus dopant concentration for the fundamental peak ($2\theta = 17.0–18.5°$).

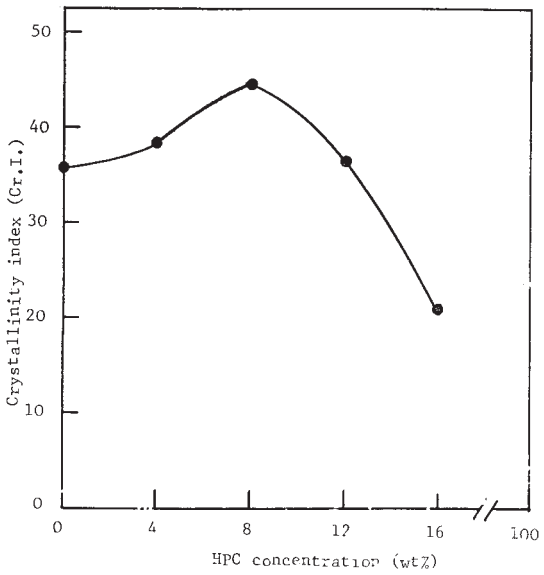

Figure 9 Variation in CrI of pure PVA and the HPC-doped PVA samples.

complicated molecular and crystalline structure induced in doping. It has been recognized that the dopant concentration plays a dominant role in both morphological and microstructural change in the polymer matrix.[39] This may have been attributed to variations in the internal mechanisms that occurred by the induced effect of doping on the structure of PVA. As a result, it produced variations in the macromolecular and micromolecular structure of the PVA network.

Spectrophotometric analysis (FTIR)

Figure 10 shows the FTIR transmittance spectra for pure PVA and the HPC-doped PVA samples as functions of wave number in the range 4000–500 cm^{-1}. The chemical assignments for pure PVA were considered and are shown in Table IV. The heights of the peaks of the assigned groups at their wave numbers shown in the spectra were taken to represent the variation in the group band intensities for different dopant concentrations and are shown in Figure 11. A clear variation was observed in the transmission bands of the PVA/HPC copolymers when compared with that shown for pure PVA.

It is well known that Transmission + Absorption + Reflection = 1; when reflection is neglected, absorption is inversely proportional to transmission. So, the absorption and optical density of the chemical groups decrease with increasing transmission. Any increase or decrease means a change in the molecular configuration of the polymer.

The transmittance band observed at 1663 cm^{-1} was attributed to the absorbtion of H_2O.[40] On the other hand, the absorption bands at 1566 and 1738 cm^{-1},

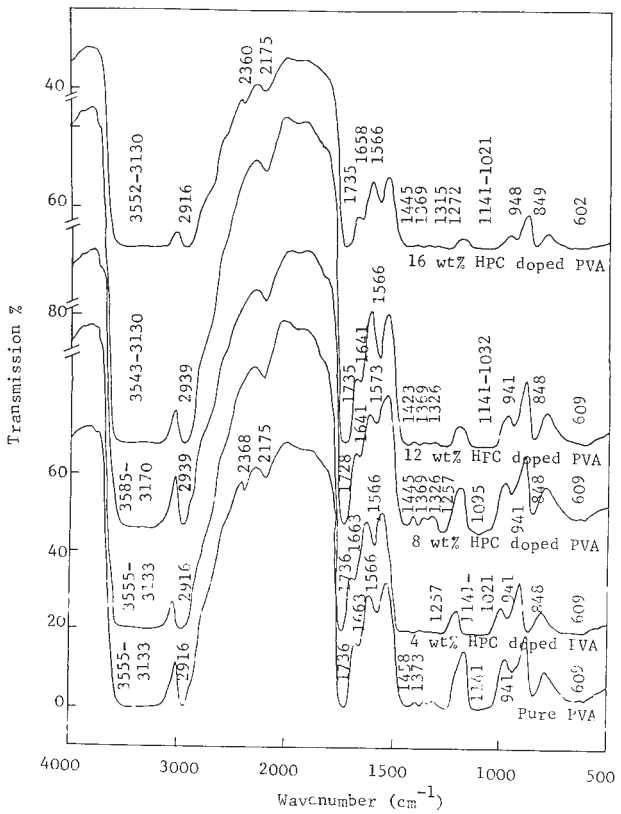

Figure 10 FTIR transmittance spectra for pure PVA and the HPC-doped PVA samples.

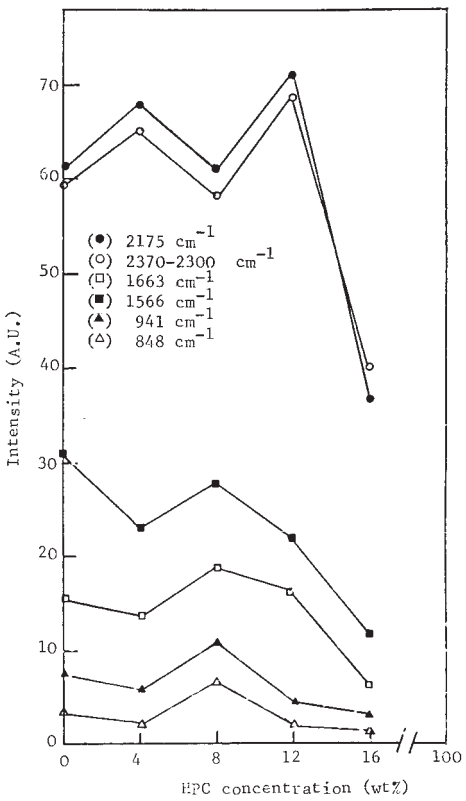

Figure 11 Variation in band intensities for some chemical groups of pure PVA and the HPC-doped PVA samples as a function of HPC dopant concentration.

assigned to the C═O group in PVA, which were likely due to the absorption of the residual acetate group,[41] clearly changed in the PVA/HPC copolymer films. It is shown in Figures 10 and 11 and Table IV that the intensities of all of the groups, except those with bands at about 2368 and 2175 cm^{-1} for the sample with 4 wt

TABLE IV
Positions and Assignments of the Most Absorption Bands of Pure and HPC-Doped PVA Samples

Wavenumber (cm^{-1})						
Pure PVA	4 wt % HPC	8 wt % HPC	12 wt % HPC	16 wt % HPC	Assignments	Refs.
3555–3133	3555–3133	3585–3170	3543–3130	3552–3130	Hydrogen-bonded and hydroxyl (O—H) group	42 and 47
2916	2916	2939	2939	2916	C—H stretching vibration	41, 42 and 47
2368	2368	2347	2369	2360	Hydroxyl (O—H) group	48
2175	2175	2175	2130	2175	Fundamental band CO	
1736	1736	1728	1735	1735	Carbonyl-group (C═O) stretching	41, 42, and 47
1663	1663	1641	1641	1658	Water absorption and C═O stretching	40, 42, and 43
1566	1566	1573	1566	1566	Carbonyl group (C═O)	41, 42, and 43
1458–1431	1458–1431	1445	1423	1445	O—H, C—H bending, and —CH_2 deformation	43
1373	1373	1369	1369	1369	—CH_2 wagging	43
1334	1336	1326	1326	1315	C—H bending	47
1275–1236	1257	1257	1257	1272	O—H bending and C—H wagging	43
1141–1021	1141–1021	1095	1141–1032	1141–1021	C—O stretching vibration	43
941	941	941	941	948	Skeletal and —CH_2 rocking	43
848	848	848	848	849	Skeletal and —CH_2 rocking	43
609	609	609	609	602	O—H twisting	47

% HPC, dropped by about 50–87% of the value for pure PVA. This spectral changes resulted from the incorporation of HPC into PVA and may have been due to the lower percentage of HPC added to PVA, the occurrence of CH_2 groups in the structure of PVA, or both factors.[42] By following the FTIR spectra in the neighborhood of 3400 cm^{-1} (3600–3100 cm^{-1}) in Figure 10, we easily assigned the observed strong band as OH— stretching vibrations.[43] The variation of this band intensity with increasing HPC content may have allowed us to specify a strong or weak interaction between HPC ions and the O—H stretching groups belonging to different chains in PVA.[44] The presence of hydrogen-bonded structures in some polymers could be inferred at once from the presence of the bond form of the hydrogen stretching mode. Thus, in PVA, the OH band at 3400 cm^{-1} showed that the molecular chains formed hydrogen bonds. The IR spectra in Figure 10 were completely absorbed in the OH— stretching (3400 cm^{-1}; Transmission = 0) for all of the samples. Moreover, O—H groups are polar groups, and the accessibility for polar groups is of great importance in polymer modification (especially in fabrication). The position and the bonding of these groups are influenced by crystallinity and crystal modification.

Furthermore, a decrease in transmittance of carbonyl groups indicates a decrease in their growth, which may suggest that they are converted into volatile compounds.[45] A decrease in carbonyl groups can be related to the enhancement of some mechanical properties of the polymers. The shape of the carbonyl band at 1736 cm^{-1}, as shown in Figure 10, indicated a change in the balance of free and associated carbonyl groups in the blend. The hydroxyl and carbonyl stretching vibration bands are affected by hydrogen-bonding interactions and are most amenable to quantitative analysis.

With respect to the two groups at 2175 and 2370–2300 cm^{-1}, they were assigned as the fundamental band CO and OH groups, respectively (Table IV). It is dear from Figure 11 that different trends for these groups were followed, and their peak heights had wavy shapes. These trends may explain that there was an interchange between the fundamental band CO at 2175 $^{-1}$ and the bands at 1663 and 1566 cm^{-1} (C═O stretching and C═O). In addition, the appearance and change of the band around 2368 cm^{-1} could have been related to the change in the intensity of the broad band at about 3400 cm^{-1}, which was interpreted as a hydrogen-bonded OH— stretching mode.

Visual inspection

A common qualitative technique for the estimation of blend miscibility is visual inspection. A clear and transparent film is produced if the blend is a miscible and compatible one. Films of immiscible blends are usually diffuse and opaque. Sometimes, optical transparency fails to assure miscibility because blend constituents may have matching refractive indices.[46] All of the samples under investigation were fully transparent and clear and had no change in color. This is a symptom of compatibility.

CONCLUSIONS

From these results, we concluded that

1. The investigation of the effects of doping on PVA by HPC was important; doping altered PVA's physical and chemical properties to different degrees, so improvement in its commercial and medical applications could be obtained.
2. The use of many techniques (thermal analysis, XRD, and FTIR) clarified the changes in the host polymer (PVA) structure, which provided additional information about the mechanism of doping-induced changes at different concentrations of the dopant polymer.
3. Changes in the properties of the host polymer depend on the chemical nature of the dopant polymers and the way in which they interact with the host matrix.
4. Thermal characterization gave a fairly good idea of the changes taking place in the PVA polymer. The variation in shape and area of endothermic peaks indicated changes in T_g, T_m, and average crystallite size and showed the effects on the crystalline regions.
5. XRD analyses showed the broadening and sharpening of peaks at different dopant concentrations of HPC, which confirmed changes in the crystallinity/amorphosity ratio and crystallite size.
6. As shown by the FTIR results, it was clear that an increase in dopant concentration changed the chemical bonds and, hence, changed the molecular configuration of PVA. This is shown by the pronounced variation in the intensity of transmission bands and little shift in the band positions.

References

1. Shamash, K. Text Mon 1989, 15, 16.
2. Rigby, A. J.; Anand, S. C.; Horrocks, A. R. In Proceedings of the Medical Textiles 96 Conference, Bolton Institute; Bolton: Lanes, England, 1996; p 83.
3. Tager, A. Physical Chemistry of Polymers; Mir Publishers: Moscow, 1972.
4. Martien, F. L. Encyclopedia of Polymer Science and Engineering; Wiley: New York, 1986; p 167.
5. Finch, C. A. Poly(vinyl alcohol) Development; Wiley: Chichester, England, 1992; p 18.

6. Hodge, R. M.; Edward, G. H.; Simon, G. P. Polymer 1996, 37, 1371.
7. Muhlebach, A.; Muller, B.; Pharis, C.; Hofmann, M.; Seiferling, B.; Guerry, D. J Polym Sci Part A: Polym Chem 1997, 35, 3603.
8. Carraher, C. L. E.; Moore, J. Modification of Polymers; Plenum: New York, 1983; p 105.
9. Saxena, A. K.; Marler, J.; Benvenuto, M.; Willital, G. H.; Vacanti, J. P. Tissue Engineering 1999, 5, 525.
10. Kim, S. S.; Kaihara, S.; Benvenuto, M. S.; Kim, B. S.; Mooney, D. J.; Vacanti, J. P. J Pediatr Surg 1999, 34, 124.
11. Peppas, N. P.; Merril, E. W. J Biomed Mater Res 1977, 11, 423.
12. Deitzel, J. M.; Kleinmeyer, J.; Harris, D.; Becktan, N. C. Polymer 2001, 42, 261.
13. Caro, V.; Paik Sung, C. S.; Merril, E. W. J Appl Polym Sci 1976, 20, 3241.
14. Grubb, D. T.; Kearney, F. R. J Appl Polym Sci 1990, 39, 695.
15. Huang, R. Y. M.; Rhim, J. W. Polym Int 1993, 30, 129.
16. Langer, R. S.; Peppas, N. A. Biomaterial 1981, 2, 201.
17. Sharma, A. K.; Rukmini, B.; Santhi Sager, D. Mater Lett 1991, 12, 59.
18. Nalwa, H. S. J Mater Sci 1992, 27, 210.
19. Venugopal Reddy, N.; Nakasimha, V. V. R. J Mater Sci Lett 1992, 11, 1036.
20. Basha, A. F.; Badawy, M. E. Proc Math Phys Soc Egypt 1987, 63, 79.
21. Segal, L.; Creely, I. S.; Martin, A. E.; Conard, C. M. Text Res J 1959, 29, 786.
22. Gullis, C. F.; Hirshler, M. M. The Combustion of Organic Polymers; Clarendon: Oxford, 1981; p 117.
23. Anders, H.; Zimmerman, H. Polym Degrad Stab 1987, 8, 111.
24. Cryghton, J. S.; Holmes, D. A. In Proceedings of the Third ICTA Conference, Davos, Switzerland: Thermal Analysis, 1971; Vol. 3, p 411.
25. Chiu, J. J Polym Sci Part C: Polym Symp 1966, 2, 25.
26. Basha, A. F.; Amin, M.; Darwish, K. A.; Abdel Samed, H. A. J Polym Mater 1988, 5, 115.
27. Garrett, P. D.; Grubb, D. T. J Polym Sci Polym Phys Ed 1988, 26, 2509.
28. Karasz, F. E. In Polymer Blends and Mixtures; Walsh, D. J.; Higgins, J. S.; Maconnachie, A. NATOASI Series E, Applied Sciences No. 89; Nijhoff: The Hague, The Netherlands, 1985; p 25.
29. Gordon, M.; Taylor, J. S. J Appl Chem 1952, 2, 493.
30. Fox, T. G. Bull Am Phys Soc 1956, 1, 123.
31. Gireco, R. In Polymer Blends and Mixtures; Walsh, D. J.; Higgins, J. S.; Maconnachie, A. NATOASI Series E, Applied Sciences No. 89; Nijhoff: The Hague, The Netherlands, 1985; p 453.
32. Ciemniecki, S. L.; Glasser, W. G. Polymer 1988, 20, 1030.
33. Hammel, R.; MacKnight, W. J.; Karasz, F. E. J Appl Phys 1975, 46, 4199.
34. Wenig, W.; Karasz, F. E.; MacKnight, W. J. J Appl Phys 1975, 46, 4166.
35. Kotelnikova, N. E. Cellulosics, Chemical, Biochemical and Material Aspects; Ellis Horwood: Hemel Hempstead, England, 1993.
36. Atella, R. C. Advances in X-Ray Analysis; Plenum and University of Denver, Canada: 1962; p 104.
37. Philips, P. J. Electrical Properties of Solid Insulating Materials; ASTM Book Series of Engineering Dielectrics VII; American Society of Testing and Materials: West Conshohocken, PA, 1980.
38. Kagjiya, T.; Nishimoto, S.; Watanobe, Y.; Kato, M. Polym Degrad Stab 1985, 12, 261.
39. Garrett, P. D.; Grubb, D. T. Phys Rev B 1980, 22, 2099.
40. Bravar, M.; Rek, V.; Kostela-Biffi, R. J Polym Sci Polym Symp 1973, 40, 19.
41. Pritchard, J. G. Poly(vinyl alcohol) Basic Properties and Uses; Gordon and Breach: New York, 1970.
42. Ibrahim, A. S.; Attia, G.; Abo-Ellil, M. S.; Abd El-Kader, F. H. J Appl Polym Sci 1997, 63, 343.
43. Liang, C. Y.; Pearson, F. G. J Polym Sci 1959, 25, 303.
44. Pritchard, J. G.; Nelson, H. M. J Phys Chem 1960, 64, 795.
45. De Sai, R. L.; Shield, J. A. Makromol Chem (Basel) 1969, 122, 134.
46. Yu, A. J. In Copolymers, Polyblends and Composites; Platzer, N. A. J., Ed.; Advances in Chemistry Series 142; American Chemical Society: Washington, DC, 1975.
47. Smith, A. L. Applied Infrared Spectroscopy, Fundamentals Techniques and Analytical Problem-Solving; Wiley: New York, 1979.
48. Fadel, M. A.; Osiris, W. G.; Abou El-Ela, K. S.; Mostafa, A. M. A.; Hussein, A. M. Egypt J Biophys 1998, 4, 103.